Electronic Supporting Information

Totally atom-economical synthesis of lactic acid from formaldehyde: combined bio-carboligation and chemo-rearrangement without the isolation of intermediate

Tianzhen Li, ‡[a,b] Zijing Tang, ‡[b] Hongli Wei, ‡[b] Zijian Tan,[b] Pi Liu,[b] Jinlong Li,[b] Yingying Zheng,[b] Jianping Lin,[b] Weidong Liu,[b] Huifeng Jiang,[b] Haifeng Liu,*[c] Leilei Zhu,*[b] and Yanhe Ma[b]

Corresponding Author:
haifeng.liu@uni-graz.at;
zhu_ll@tib.cas.cn

Table of Contents

SUPPORTING INFORMATION

1. Experimental Procedures

1.1 Materials and methods

All analytical-reagent grades or even higher quality chemicals were purchased from Sinopharm (Beijing, China) and Yuanye Biological (Shanghai, China), except the resins (GE Healthcare, Boston, USA) for purifications. EasyTaq DHA polymerase and FastPfu DNA polymerase were purchased from TransGen Biotech (Beijing, China), and Dpn I was purchased from New England Biolabs (Beverly, MA, USA). Galactose oxidase (GalOD) was purchased from Yuanye Biological (Shanghai, China) and Aladdin (Shanghai, China), Horseradish peroxidase (HRP) was purchased from GENVIEW (USA), 2,2'-azino-bis(3-ethylbenzothiazoline-6-sulfonate) (ABTS) was purchased from Coolaber (Beijing, China), Oligonucleotide syntheses and DNA sequencing analyses were carried out by Genewiz (Tianjin, China). The amount of DNA in cloning experiments was quantified by TECAN microplate reader (Infinite M200, TECAN, Switzerland). The formolase variant M3 (W86R/N87T/L109G/L110E/A460M) was provided by Professor Huifeng Jiang (Tianjin institute of industrial biotechnology, Chinese academy of sciences, Tianjin, China).

1.2 Construction of formolase error-prone PCR (epPCR) libraries

EpPCR libraries were generated by the standard epPCR method using parent M3 (W86R/N87T/L109G/L110E/A460M) as template. For the mutagenic PCR (95°C for 2 min, 1 cycle; 95°C, 20 s/60°C, 20 s/72°C, 3 min, 25 cycles; 72°C for 5 min, 1 cycle). EasyTaq DHA polymerase (2.5 U), dNTP mix (0.20 mM), template (25 ng, pET28a harboring the M3 gene), $MnCl_2$ (0.05 and 0.08 mM), and primers (forward: 5'-CCGCGCGGCAGCCATATG-3', reverse: 5'-GGTGGTGGTGGTGGTGCTCGAGTTATT-3', 10 pmol each) were used. The epPCR products were purified by using a TransGen PCR purification kit (TransGen Biotech, Beijing, China). The purified epPCR products were cloned into expression plasmid pET28a and transformed into *Escherichia coli* BL21-Gold (DE3) cells for further expression and screening.

1.3 Cultivation and expression of formolase variants in 96-well plates

Clones grown on LB agar plates (50 μg/mL kanamycin) were transferred into 96-well microtiter plates (V-bottomed, polystyrene plates; Beyotime, Shanghai, China) containing 150 μL LB liquid medium (50 μg/mL kanamycin). After overnight cultivation in a microtiter plate shaker (37°C, 800 rpm; Zhichu Instrument, Shanghai, China), each well was replicated by a replicator into a second series of 96-well microtiter plates containing 200 μL LB liquid medium (50 μg/mL kanamycin) and 0.1 mM Isopropyl β-D-Thiogalactoside (IPTG). All the 96-well microtiter plates were cultivated in the microtiter plate shaker at 800 rpm under 37°C for the first 4 h and then cultivated at 30°C for next 24 h. After expression, the pellets were harvested in V-bottom 96-well microtiter plates after centrifugation (4°C, 3400 rpm, 15 min; Eppendorf Centrifuge 5810 R; Eppendorf Corporate, Hamburg, German) and then resuspended in 200 μL phosphate buffer (50 mM K_2HPO_4 and KH_2PO_4, 5 mM $MgSO_4$, pH 7.4). After centrifugation, 96-well microtiter plates were stored at -20°C for following screening.

1.4 Library screening for improved activity and thermal resistance

For activity screening, the cell pellets in 96-well microtiter plates were resuspended in phosphate buffer (50 mM K_2HPO_4 and KH_2PO_4, 5 mM $MgSO_4$, pH 7.4, 50 μL), then 50 μL formaldehyde solution (phosphate buffer containing different concentrations of formaldehyde and 1mM thiamine diphosphate (TPP), pH 7.4) was added in above plates. The plates were incubated at 30°C. After incubation, the plates were centrifuged (4°C, 3400 rpm, 10 min) and supernatant was transferred into 96-well microtiter plates (flat-bottomed, polystyrene plates; Beyotime, Shanghai, China). Then assay buffer A (0.2 mg/mL GalOD, 24 U/mL HRP, 50 mM K_2HPO_4 and KH_2PO_4, 5 mM $MgSO_4$, pH 7.4, 60 μL) and assay buffer B (4 mM ABTS, 50 mM K_2HPO_4 and KH_2PO_4, 5 mM $MgSO_4$, pH 7.4, 50 μL) were added in the plates successively. The plates were immediately measured at 410 nm for 20 min using a microtiter plate reader (VersaMax; Molecular Devices, Sunnyvale, USA).

For thermal resistance screening, the variants in 96-well microtiter plates were resuspended in phosphate buffer (50 mM K_2HPO_4 and KH_2PO_4, 5 mM $MgSO_4$, pH 7.4, 50 μL) and incubated at 50°C for 30 min, then formaldehyde solution (20 mM formaldehyde, 1 mM TPP, 50 mM K_2HPO_4 and KH_2PO_4, 5 mM $MgSO_4$, pH 7.4, 50 μL) was added in above plates. The plates were then incubated in the microtiter plate shaker at 800 rpm under 30°C. After incubation, the same procedure as above was performed for the quantification of the product DHA.

1.5 Expression of formolase variants in shaking flask and purification

Single clone was inoculated into 5 mL LB liquid medium (50 μg/mL kanamycin) and grown overnight. The cell cultures were transferred into 100 mL LB liquid medium (50 μg/mL kanamycin) with the ratio of 1:100. All the flasks were shaken at 200 rpm at 37°C. When the optical density at 600 nm (OD_{600}) reached 0.6-0.8, gene expressions were induced using 0.1 mM IPTG at 30°C for 24 h. Subsequently, *E. coli* cells were harvested by centrifugation (4°C, 4000 rpm, 15 min) and resuspended in 25 mL phosphate buffer (50 mM K_2HPO_4 and KH_2PO_4, 5 mM $MgSO_4$, pH 7.4), and subsequently followed by disruption with a low temperature ultra-high pressure continuous flow cell disrupter (LN-3000plus; JNBIO, Guangzhou, China). The disrupted cells were centrifuged (4°C, 6000 rpm, 20 min), and the supernatants were further filtered through millipore express membrane filters (0.45 μm; Sterile Millex Filter Unit; Merck kGaA, Darmstadt, Germany). The filtered cell lysates were purified by His-Spin protein mini-prep columns. Purified formolase variants protein was subsequently concentrated and purification in a centrifugal filter unit (Amicon Ultra-15 10 kDa Centrifugal Filter Devices; Merck kGaA, Darmstadt, Germany). The concentration of protein was determined using a protein assay kit (Micro BCA Protein Assay Kit; Sangon Biotech, Shanghai, China) with BSA as the standard. The homogeneity of the purified sample was controlled by sodium dodecyl sulfate polyacrylamide gel electrophoresis (SDS-PAGE) by using standard molecular biology techniques.

1.6 Kinetic characterization of parent M3 and improved variants

The k_{cat} and K_{half} values were determined from initial-velocity data measured as a function of substrate concentration. First, 50 μL different concentration of substrate solution was added in 96-well microtiter plates. Enzyme reactions were initiated by the addition of equal volume purified formolase variants. Samples were incubated at 30°C and taken out at different time points. The samples were diluted

to the linear detection range of DHA with phosphate buffer (50 mM K_2HPO_4 and KH_2PO_4, 5 mM $MgSO_4$, pH 7.4), and then were determined as followings: 90 μL reaction solution after dilution was transferred to a 96-well microtiter plate, 60 μL assay solution A (0.3 mg/mL GalOD, 36 U/mL HRP, 50 mM K_2HPO_4 and KH_2PO_4, 5 mM $MgSO_4$, pH 7.4) was added in the plate, and then 50 μL solution B (3.2 mM ABTS, 50 mM K_2HPO_4 and KH_2PO_4, 5 mM $MgSO_4$, pH 7.4) was added in the plates. The plates were immediately measured at 410 nm for 20 min by using a microtiter plate reader. The initial-velocity data was fitted to allosteric sigmoidal equation ($v=V_{max}\times S^n/(K_{half}{}^n+S^n)$), where v is the initial enzyme velocity, S is substrate concentration, V_{max} is the maximum enzyme velocity, K_{half} is the ligand concentration at which half of the active sites are occupied (concentration of half saturation). All experiments were conducted in triplicate.

1.7 Analysis of GA and DHA generated by parent M3 and improved variants

Parent M3 and variants M4, M5, M6 were purified and quantized, GA and DHA in reaction mixtures were detected by microtiter plate reader as following: 100 μL reaction solution comprised 0.027 mM of purified enzyme, 100 mM formaldehyde, 0.5 mM TPP, 50 mM K_2HPO_4 and KH_2PO_4, 5 mM $MgSO_4$, pH 7.4. After incubation at 30°C for 3 h, 30 μL reaction solution after dilution with phosphate buffer was transferred to a 96-well microtiter plate and added 150 μL the buffer (1.5 g diphenylamine was dissolved in 100 mL acetic acid and then added 1.5 mL H_2SO_4) for the detection of GA, the plate was cultured at 90°C for 30 min, subsequently was detected at 650 nm. 30 μL reaction solution was transferred to another 96-well microtiter plate and 60 μL phosphate buffer was added, the quantity of DHA was detected at 410nm.

1.8 Thermal resistance profiles of parent M3 and improved variants

Thermal inactivation of parent M3 and variants M5 and M6 was monitored by activity measurements after heat treatment. Purified M3, M5 and M6 in phosphate buffer (50 mM K_2HPO_4 and KH_2PO_4, 5 mM $MgSO_4$, pH 7.4) were incubated at a range from 36°C to 65°C for 4 h. Subsequently, equal volume of formaldehyde solution (200 mM formaldehyde, 1 mM TPP in phosphate buffer for M3, M5; 400 mM formaldehyde, 1 mM TPP in phosphate buffer for M6) was added in above each sample and cultured at 30°C for 3 h. The quantity of DHA was detected at 410nm and assayed for residual activity. The T_m value was defined as the temperature at which 50% of the initial enzyme activity was decreased after heat treatment.

1.9 Structural integrity of parent M3 and improved variants at various temperatures by CD measurements

The CD spectra (from 190 to 240 nm) was measured with a Circle Dichromatic Spectrometer (Chirascan: Applied Photophysics Ltd; Leatherhead, England) under a constant nitrogen flow, with spectra ranged from 190-240 nm by using a 1 mm path-length cell and a 1 nm bandwidth. Each spectrum was shown as the average of two individual measurements. The collected raw data were converted into delta epsilon (De, molar circular dichroism). Purified M3 and variants M5 and M6 were first incubated for 4 h at five temperatures: 36.0°C, 40.0°C, 45.0°C, 50.0°C and 55.0°C, and then subjected to CD measurement. Baseline measurements were determined in phosphate buffer (50 mM K_2HPO_4 and KH_2PO_4, 5 mM $MgSO_4$, pH 7.4) and subtracted from the experimental data. CD data were analyzed by using CDToolX software and Dichroweb website (http://dichroweb.cryst.bbk.ac.uk) to derive the α-helical content.

1.10 The synthesis of lactic acid from commercial DHA by four hydroxides

25 mL DHA solution (100 mM) was dropwise added into 250 mL round-bottom flask containing 25 mL hydroxide (5 M NaOH or KOH solution or 250 mM $Ba(OH)_2$ or $Ca(OH)_2$ suspension), stirred by Magnetic rotor at room temperature. After 24 h, reaction mixture was acidified with dilute sulfuric acid to pH 1-2. Experiments were replicated at least 3 times.

The HPLC system was carried out on an Agilent 1260 system equipped with Aminex HPX-87H column (Bio-Rad). (A) production detection of the reaction catalyzed by NaOH or KOH: refractory index (RI) detector ; mobile phase: 10 mM H_2SO_4, flow rate: 0.5 mL/min, sample volume: 20 μL, column temperature: 35°C; (B) production detection of the reaction catalyzed by $Ba(OH)_2$ or $Ca(OH)_2$: UV detector (210 nm), mobile phase: 2.5 mM H_2SO_4, flow rate: 0.5 mL/min, sample volume: 20 μL, column temperature: 65°C.

1.11 The chemoenzymatic synthesis of lactic acid from formaldehyde

Enzymatic carboligation reaction (total volume 20 mL) was executed in 50 mL falcon tube containing fomolase variant M6 (0.135 mM), formaldehyde (300 mM), TPP (0.5 mM), $MgSO_4$ (5 mM) and phosphate buffer (50 mM K_2HPO_4 and KH_2PO_4, pH 7.4). The reaction was conducted at 30°C, 220 rpm for 1 h. After removing the enzymes used in the carboligation step through ultrafiltration, 17.5 mL reaction mixture in a separatory funnel was added dropwise into a 250 mL round-bottom flask containing NaOH (17.5 mL, 5 M) under stirred condition. After 19 h, reaction mixture was acidified with dilute sulfuric acid to pH 1-2 for HPLC analysis.

The HPLC system was carried out on an Agilent 1260 system equipped with Aminex HPX-87H column (Bio-Rad). (A) production detection of the reaction catalyzed by formolase for the first step: UV detector (210 nm); mobile phase: 10 mM H_2SO_4, flow rate: 0.5 mL/min, sample volume: 20 μL, column temperature: 35°C; (B) production detection of the reaction catalyzed by NaOH for the second step : both UV detector (210 nm) and RI detector, mobile phase: 10 mM H_2SO_4, flow rate: 0.5 mL/min, sample volume: 20 μL, column temperature: 35°C.

Atom economy = (molecular mass of desired product / molecular mass of all reactants) × 100. Atom economy of lactic acid from formaldehyde = (molecular mass of lactic acid) / (3×molecular mass of formaldehyde) × 100.

1.12Protein purification of formolase variants for crystallization

Parent M3 and variant M6 Cells were cultured in shaking flask and harvested as mentioned in above, and then resuspended in buffer containing 25 mM Tris-HCl, 150 mM NaCl, 20 mM imidazole, pH 7.5, followed by disruption with a low temperature ultra-high pressure continuous flow cell disrupter. Cell lysates were centrifuged (4°C, 15000 rpm, 1 h) and the supernatants were harvested. The purification procedure was carried out at 4°C as following: the supernatants were applied to a Ni-NTA column fast protein liquid chromatography (FPLC) system (GE Healthcare), the target proteins eluted at ~100 mM imidazole when using a 20-250 mM imidazole gradient. The purified protein fractions were run on SDS-PAGE to ascertain the size and purity. On the SDS-PAGE, formolases showed one clear band at MW 56 kDa.

Proteins were concentrated to a volume of 3 mL and applied to a size exclusion column (Saphacryl S-200 26/60, 320 mL, GE Healthcare) equilibrated with gel filtration buffer (25 mM Tris-HCl, 500 mM NaCl, pH 7.5) at a flow rate of 1 mL/min. Analyzed by a SDS-PAGE, component of the peak eluted at ~60 mL which contained formolase proteins were collected. The purified proteins were concentrated to 10 mg/mL in buffer (25 mM Tris-HCl, 500 mM NaCl, pH 7.5).

1.13Crystallization, data collection, structure determination and refinement of formolase variants

The crystal of M3 was obtained using No.38 of Memstart screen kit (Molecular Dimensions) (0.1 M sodium acetate 4.6, 0.1 M sodium chloride, 12 % w/v PEG 6000), the crystal of M6 was obtained using No.45 of Cryo II screen kit (Emerald Biosystems) (0.1 M acetate pH 4.5, 0.2 M NaCl,40% (v/v) PEG-300). All the crystals were obtained with the sitting-drop vapor method. In general, 1 µL 5 mg/mL formolase was mixed with 1 µL of reservoir solution in 48-well Cryschem plates, then equilibrated against 100 µL of the reservoir at 25°C. Within 2 to 3 days, the crystals reached dimensions suitable for X-ray diffraction.

All of the X-ray diffraction data sets were collected at beam lines BL17U1, BL17B1, BL18U1 and BL19U1 of the Shanghai Synchrotron Radiation Facility (SSRF) and National Facility for Protein Science (NFPS) in Shanghai. The crystals were mounted in a cryoloop and soaked with cryoprotectant solution (adding 5-10% glycerol in protein crystallization condition), prior to data collection at 100 K. The diffraction images were processed by using HKL2000[2]. The crystal structures of these mutants were all solved by molecular replacement (MR) method with Phaser[3] from the CCP4 suite [4] using the structure of benzoylformate decarboxylases wild type (BFD-WT) from *Pseudomonas putida* (PDB ID code 6A50) as a search model, most of the residues were built by using ARP/wARP[5], the further manual model building and refinement was carried out using Refmac5[6] and Coot[7]. Prior to structural refinements, 5% randomly selected reflections were set aside for calculating Rfree as a monitor[8]. The 2Fo-Fc difference Fourier map showed clear electron densities for most amino acid residues. Subsequent refinements by incorporating ligands and water molecules were according to 1.0 σ map level. All figures were prepared by using the PyMOL program (http://pymol.sourceforge.net/).

1.14 Molecular docking

Molecular docking was performed using Schrödinger2018 software[9]. Crystal structure of M3 (PDB ID: 6M2Z) and variant M6 (PDB ID: 6M2Y) without TPP were used as receptor proteins. TPP-GA complex was used as ligand. Protein structures were preprocessed using Protein Preparation Wizard module in Schrödinger software. All the water molecules were deleted and missing side chains were filled using Prime. Receptor Grid was generated at the centroid of the ligand TPP and the outer box size was set to 30 X 30 X 30 Å. Glide SP[10] of docking algorithm was employed to perform all the molecular docking studies with no constraint.

1.15Molecular dynamic (MD) simulation and bind free energy calculation

The 3D structural complexes of M3-TPP-GA and M6-TPP-GA were constructed based on the optimal results of molecular docking using Schrödinger2018. Energy minimization of the constructed complexes were done using AMBER18.[11] AMBER18 was used to carry out MD simulation of final model using ff14SB force field. The 100 ns MD trajectories were further analyzed including for binding free energy calculation and the identification of relevant binding poses. The final 100 snapshots with an interval of 20 ps were extracted to the free energy calculation. The ligand (TPP-GA) binding free energy and the interaction free energy between the two monomeric chains of parent M3 and variant M6 were calculated using molecular dynamic simulation and molecular mechanics/generalized born surface area (MM-GBSA) analysis method.

$$\Delta G = \Delta E_{MM} + \Delta G_{solv} - T \cdot \Delta S = \Delta E_{bat} + \Delta E_{vdw} + \Delta E_{coul} + \Delta G_{solv.p} + \Delta G_{solv.np} - T \cdot \Delta S$$

where E_{MM} is a gas-phase MM energy, including E_{bat} (the sum of bond, angle, and torsion terms in the force field), E_{vdw} (a Van der Waals term), and E_{coul} (a coulombic term); $G_{solv.p}$ is the polar contribution to the free energy of solvation, often computed via the Generalized-Born (GB) approximation; $G_{solv.np}$ is the nonpolar free energy of solvation, which is computed as a linear function of the solvent-accessible surface area. The free energy for each species (ligand, receptor, and complex) was decomposed into a gas-phase MM energy that contained polar and nonpolar solvation terms and an entropy term (which was neglected due to the expensive computational cost and the significant uncertainty in the results). Only E_{MM} and G_{solv} were considered for the ligand binding energy calculation of TPP-GA and the E_{vdw} and E_{coul} were considered for the interaction energy calculation between the two monomeric chains.

2. Results and Discussion (Supporting)

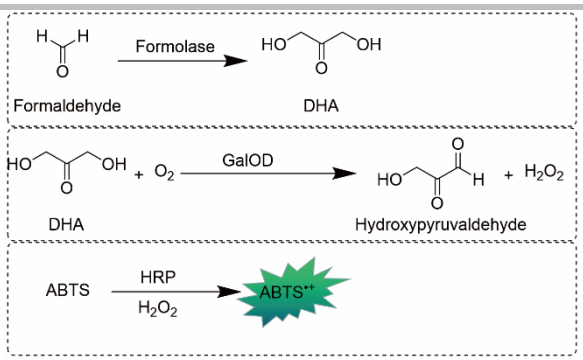

Scheme S1. Coupled enzyme assay for formolase library screening.

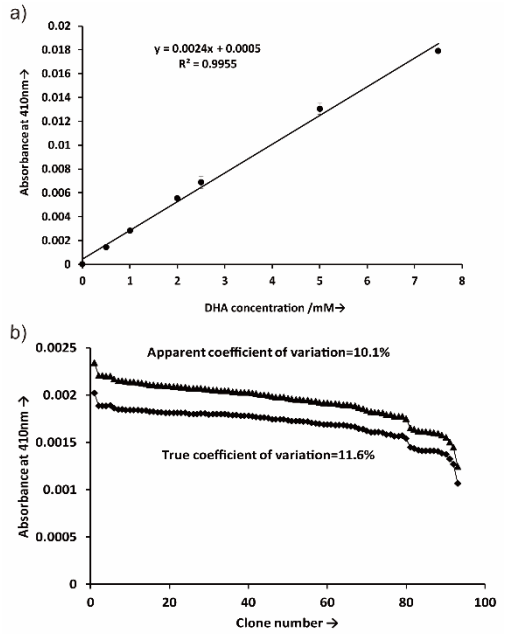

Figure S1. (a) Calibration curve of 96-well microtiter-plate-format DHA colorimetric screening assay. (b) Activity value in descending order of the parent M3 converting formaldehyde to DHA in a 96-well microtiter plate by using optimized assay protocol. The apparent coefficient of variation was calculated without subtracting the background, and the true coefficient of variation was calculated after background subtraction.

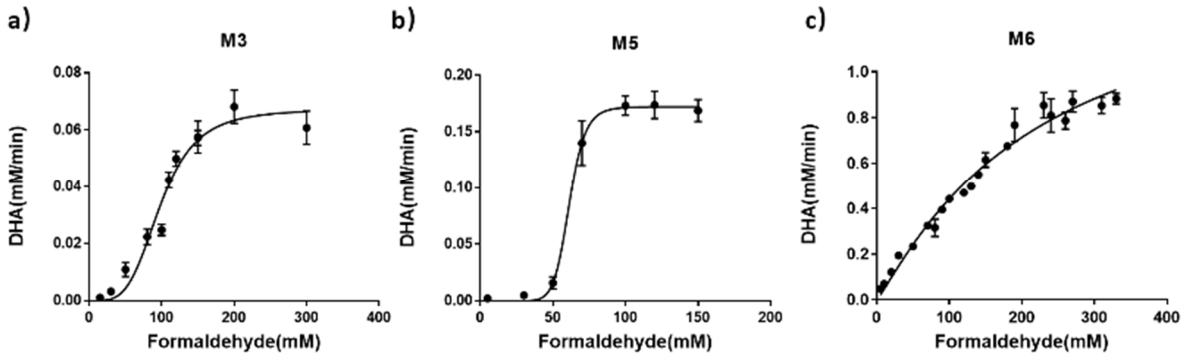

Figure S2. Enzyme kinetics of parent M3 (a), variants M5 (b) and M6 (c). Enzyme kinetics were determined with 0.060 mM enzyme.

Table S1. Percentage of α-helical content of parent M3, variants M5 and M6 after heat inactivation (4 h, 50 mM K_2HPO_4 and KH_2PO_4, 5 mM $MgSO_4$, pH 7.4) at varied temperature.

Variants	α-helical content (%)				
	36°C	40°C	45°C	50°C	55°C
M3 (parent)	23.8	18.1	3.5	3.1	3.0
M5	24.2	16.8	9.8	5.0	4.2
M6	23.8	21.8	16.0	9.1	9.4

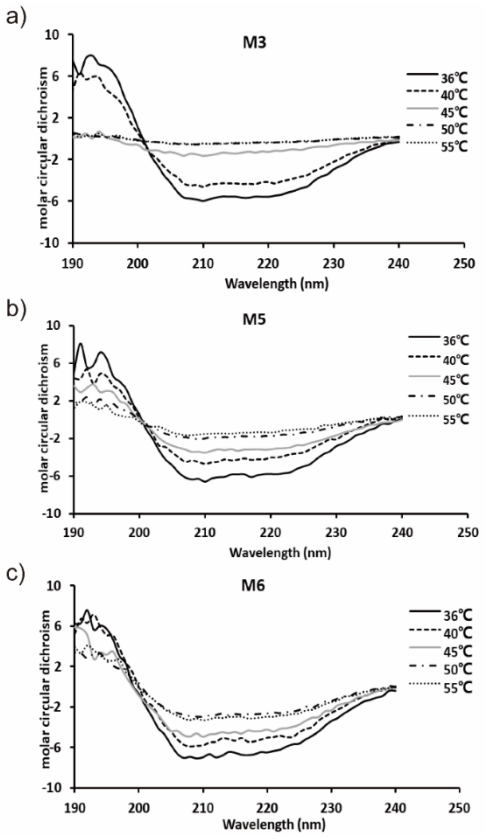

Figure S3. CD spectrum of M3 (a), M5 (b) and M6 (c) after incubation at various temperature (36°C, 40°C, 45°C, 50°C and 55°C)

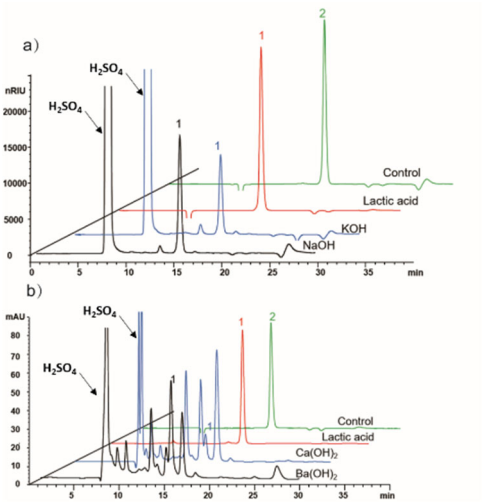

Figure S4. HPLC chromatogram of lactic acid converted from commercial DHA by four hydroxides. (a) HPLC chromatogram of lactic acid from DHA promoted by NaOH and KOH. The black line represents reaction sample promoted by NaOH, the blue line represents reaction sample promoted by KOH, the red line represents lactic acid standard, the green line represents control without hydroxides, the number 1 is lactic acid and the number 2 is DHA. (b) HPLC chromatogram of lactic acid from DHA promoted by $Ba(OH)_2$ and $Ca(OH)_2$. The black line represents reaction sample promoted by $Ba(OH)_2$, the blue line represents reaction sample promoted by $Ca(OH)_2$, the red line represents lactic acid standard, the green line represents control without hydroxides, the number 1 is lactic acid, the number 2 is DHA. All experiments were executed using 50 mM DHA at room temperature for 24 hours.

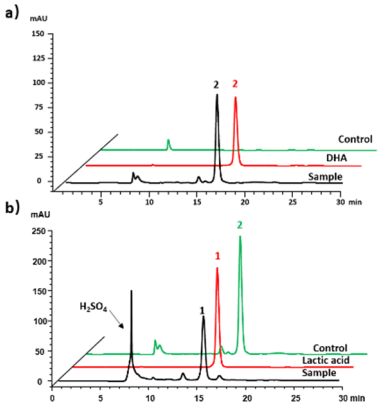

Figure S5. HPLC chromatograms of DHA and lactic acid synthesized from formaldehyde by chemoenzymatic reactions. (a) HPLC chromatogram of DHA converted from formaldehyde. The black line represents reaction sample catalyzed by M6, the red line represents the DHA standard, the green line represents the control sample without M6 and the peak number 2 is DHA. (b) HPLC chromatogram of lactic acid converted from the enzymatically synthesized DHA. The black line represents reaction sample promoted by NaOH, the red line represents lactic acid standard, the green line represents control without NaOH, the peak number 2 is DHA, the peak number 1 is lactic acid.

Table S2. The free binding energies (ΔG_{bind}) of TPP-GA and interaction free energies between the two chains of M3 or M6 during MD simulation using the MM-GBSA method. [a]

Variants	monomer-monomer	protein-TPP-GA1	protein-TPP-GA2
M3	-55.8167 ± 13.3890	-130.9157 ± 7.5487	-135.4074 ± 7.5888
M6	-84.2372 ± 12.9015	-166.1555± 10.2043	-164.4413 ± 9.1886

[a] the unit of ΔG_{bind} is kcal/mol.

3. References

1. K. Plasch, G. Hofer, W. Keller, S. Hay, D. J. Heyes, A. Dennig, S. M. Glueck and K. Faber, *Green Chem.*, 2018, **20**, 1754-1759.
2. Z. Otwinowski and W. Minor, *Methods Enzymol.*, 1997, **276**, 307-326.
3. A. J. McCoy, R. W. Grosse-Kunstleve, P. D. Adams, M. D. Winn, L. C. Storoni and R. J. Read, *J. Appl. Crystallogr.*, 2007, **40**, 658-674.
4. M. D. Winn, C. C. Ballard, K. D. Cowtan, E. J. Dodson, P. Emsley, P. R. Evans, R. M. Keegan, E. B. Krissinel, A. G. Leslie, A. McCoy, S. J. McNicholas, G. N. Murshudov, N. S. Pannu, E. A. Potterton, H. R. Powell, .R. J. Read, A. Vagin and K. S. Wilson, *Acta Crystallogr. D Biol. Crystallogr.*, 2011, **67**, 235-242.
5. S. X. Cohen, M. Ben Jelloul, F. Long, A. Vagin, P. Knipscheer, J. Lebbink, T. K. Sixma, V. S. Lamzin, G. N. Murshudov and A. Perrakis, *Acta Crystallogr. D Biol. Crystallogr.*, 2008, **64**, 49-60.
6. G. N. Murshudov, P. Skubak, A. A. Lebedev, N. S. Pannu, R. A. Steiner, R. A. Nicholls, M. D. Winn, F. Long and A. A. Vagin, *Acta Crystallogr. D Biol. Crystallogr.*, 2011, **67**, 355-367.
7. P. Emsley and K. Cowtan, *Acta Crystallogr. D Biol. Crystallogr.*, 2004, **60**, 2126-2132.
8. A. T. Brunger, *Acta Crystallogr. D Biol. Crystallogr.*, 1993, **49**, 24-36.
9. G. M. Sastry, M. Adzhigirey, T. Day, R. Annabhimoju and W. Sherman, *J. Comput. Aided Mol. Des.*, 2013, **27**, 221-234.
10. R. A. Friesner, R. B. Murphy, M. P. Repasky, L. L. Frye, J. R. Greenwood, T. A. Halgren, P. C. Sanschagrin and D. T. Mainz, *J. Med. Chem.*, 2006, **49**, 6177-6196.
11. L. F. Song, T. S. Lee, C. Zhu, D. M. York and K. M. Merz, Jr., *J. Chem. Inf. Model.*, 2019, **59**, 3128-313.